

Transcriptomic Analyses Provide Insight Into Adventitious Root Formation of *Euryodendron Excelsum* H. T. Chang During *Ex Vitro* Rooting

Yuping Xiong

South China Botanical Garden

Songjun Zeng (✉ zengsongjun@scib.ac.cn)

South China Botanical Garden

Shuangyan Chen

South China Botanical Garden

Zhenpeng Wei

Zhongkai University of Agriculture and Engineering

Xiaohong Chen

South China Botanical Garden

Beiyi Guo

South China Botanical Garden

Ting Zhang

South China Botanical Garden

Yuying Yin

South China Botanical Garden

Xincheng Yu

South China Botanical Garden

Jinhui Pang

South China Botanical Garden

Meiyun Niu

South China Botanical Garden

Xinhua Zhang

South China Botanical Garden

Yuan Li

South China Botanical Garden

Kunlin Wu

South China Botanical Garden

Lin Fang

South China Botanical Garden

Jaime A. Teixeira da Silva

Research Article

Keywords: Euryodendron excelsum H. T. Chang, Transcriptome, Adventitious roots, Hydrogen peroxide

Posted Date: October 20th, 2021

DOI: <https://doi.org/10.21203/rs.3.rs-981177/v1>

License: © ⓘ This work is licensed under a Creative Commons Attribution 4.0 International License.
[Read Full License](#)

Version of Record: A version of this preprint was published at Plant Cell, Tissue and Organ Culture (PCTOC) on January 21st, 2022. See the published version at <https://doi.org/10.1007/s11240-021-02226-9>.

Abstract

Euryodendron excelsum H. T. Chang, a critically endangered species endemic to China, is a source of valuable material for the furniture and construction industries. However, this species has some challenges associated with rooting during *in vitro* propagation that have yet to be resolved. In this study, we optimized rooting and conducted a transcriptomic analysis to appreciate its molecular mechanism, thereby promoting the practical application of *in vitro* propagation of *E. excelsum*, and providing technical support for the ecological protection of this rare and endangered species. Results showed that *ex vitro* rooting performed the highest rooting percentage with 98.33% at 25 d. During *ex vitro* rooting, there was a wide fluctuation of endogenous levels of indole-3-acetic acid (IAA) and hydrogen peroxide (H_2O_2) at the stage of root primordia formation. Transcriptome analysis revealed multiple differentially expressed genes (DEGs) involved in AR development. DEGs involved in plant hormone signal transduction, such as genes encoding auxin-induced protein, auxin-responsive protein, and IAA-amido synthetase Gretchen Hagen3, and in response to H_2O_2 , oxidative stress, abiotic and biotic stimuli were significantly up- or down-regulated by *ex vitro* treatment with 1 mM indole-3-butyric acid (IBA). Our results indicate that *ex vitro* rooting is an effective method to induce AR from *E. excelsum* plantlets during micropropagation. DEGs involved in the plant hormone signal transduction pathway played a crucial role in AR formation. H_2O_2 , produced by environmental stimulation, might be related to AR induction as a result of the synergistic action with IBA, ultimately regulating the level of endogenous IAA.

Key Message

Under *ex vitro* rooting, a synergistic action between H_2O_2 produced by environmental stimulation and IBA played crucial role in the regulation of AR formation from *E. excelsum* plantlets during micropropagation.

Introduction

Adventitious root (AR) system is one of plant roots systems that arises from parts of the plant rather than from the roots of the embryo (Barlow 1986). ARs derived from non-root tissues, are the main path by which new plantlets root in vegetative propagation, and usually generated during normal development or stress conditions (Steffens and Rasmussen 2016). *In vitro* propagation via tissue culture has become an important technology in plant conservation strategies given its advantages, such as high propagation coefficient, freedom from restrictions imposed by season, especially for rare and endangered species (Bhardwaj et al 2018, Khater and Benbouza 2019, Rameshkumar et al 2017). However, in some *in vitro* propagation systems, plants may display rooting-recalcitrance problems, for example by *Juniperus thurifera* L. (Khater and Benbouza 2019), *Zeyheria montana* Mart. (Cardoso and da Silva 2013), *Elegia capensis* (Burm. f.) Schelpe (Verstraeten and Geelen 2015), and *Cariniana legalis* (Lerin et al 2021). Rooting-related problems limit the application of *in vitro* propagation for plant breeding and conservation efforts. Therefore, AR formation during plant *in vitro* culture is a top research objective for plant asexual propagation breeders.

Plant growth regulators (PGRs) are commonly AR inducers used in *in vitro* culture, such as 1-naphthaleneacetic acid (NAA), indole-3-acetic acid (IAA) and indole-3-butyric acid (IBA), but these tend to show species- and concentration-dependent AR induction efficiency. For *Laburnum anagyroides* Medic., a low concentration of IAA, IBA or NAA induced AR normally, but high concentrations induced callus formation in shoot tips and subsequently, plant death (Timofeeva et al 2014). 0.25 or 0.5 mg/L of NAA promoted rooting during *in vitro* culture of *Cornus alba* L., while IBA had an adverse effect on root growth and even inhibited AR induction at 1.0 mg/L (Ilczuk and Jacygrad 2016). Moreover, *in vitro* rooting and *ex vitro* rooting also display some differences in AR formation. *In vitro* rooting to induce AR is always performed under aseptic conditions (Barpete et al 2014, Guo et al 2019, Nourissier and Monteuis 2008). In contrast, *ex vitro* rooting employs unrooted plantlets that are removed from aseptic *in vitro* conditions culture to induce AR in an open environment (Revathi et al 2018, Shekhawat and Manokari 2016). Although the two culture methods are affected by various factors, *ex vitro* rooting can enhance rooting percentage and survival during plant acclimatization, and reducing limiting factors in micropropagation (Benmahioul et al 2012, Yan et al 2010). For example, *Ceratonia siliqua* L. plantlets treated with 4.8 μ M IBA displayed a 46.3% rooting response, forming a fragile root system when rooted *in vitro* whereas the induction of AR from *ex vitro* shoots treated with 14.4 μ M IBA showed significantly higher rooting percentage (91.7%), and a normal morphological appearance, and were successfully acclimatized, showing more than 90% survival (Lozzi et al 2019).

The mechanism of AR induction involves various key genes, proteins, and pathways (Chen et al 2020a, Qi et al 2020, Stevens et al 2018). Most PGRs promote AR development by regulating the level of endogenous IAA, thus genes and pathways related to the biosynthesis and transport of IAA are considered to play a significant role in AR formation (Lakehal and Bellini 2019). Transcriptome sequencing revealed that candidate genes involved in AR formation of *Mangifera indica* L. cv. Zihua cotyledon segments were predicted to encode polar auxin transport carriers, auxin-regulated proteins and cell wall remodeling enzymes (Li et al 2017). In *Arabidopsis thaliana*, IBA induced AR formation in thin cell layers by conversion into IAA involving nitric oxide activity, and by positive action on IAA transport and biosynthesis (Fattorini et al 2017). Genes related to the synthesis, transport, metabolism and recognition of plant hormone were involved in the *in vitro* induction and elongation of ARs in *Populus euramericana* (Zhang et al 2019b). However, knowledge of the molecular aspects of adventitious rooting in plants, especially in woody species that are recalcitrant to rooting, remains scanty. Understanding the mechanism of AR formation is of great importance to strategize plant breeding and conservation efforts to maximize the marketable yield and research value, especially of rare and endangered plants.

Euryodendron excelsum H. T. Chang, a monotypic genus endemic to China, is fine-textured and colorful, making it a source of valuable material for the furniture and construction industries (Chang 1963). However, mainly as a result of habitat destruction and deforestation caused by human activity, only a single population of *E. excelsum* can now be found at Bajia Zhen, Yangchun County, Guangdong Province, in southern China (Shen et al 2008, Ye et al 2002). *E. excelsum* is naturally propagated only by seeds, but seed germination and seedling growth toward adulthood are fragile stages that limit natural recruitment and regeneration (Shen et al 2009, Wang et al 2002). Based on the categorization of the

International Union for Conservation of Nature and Natural Resources (IUCN), *E. excelsum* has been listed as a critically endangered plant since 1998, and continues to maintain this status and faces a high risk of extinction, implying that some strategies were put forward for the conservation of *E. excelsum* populations (Barstow 2020).

In our previous study, a micropropagation system for *E. excelsum* was established by *in vitro* culture. When treated with either IBA or NAA, *in vitro* *E. excelsum* showed lower rooting percentage in agarized woody plant medium (WPM) (Lloyd GB 1980) than in agar-free vermiculite-based WPM after culture for 2 months, and callus formed at the base of stems in these media, hampering the successful transplantation of plantlets (Chen et al 2020b). We inferred from that there may be other factors that can stimulate AR formation in *E. excelsum* when cultured *in vitro*, or that enhance the induction efficiency of PGRs. Thus, the objectives of this study were to improve the micropropagation system of *E. excelsum* by optimizing the AR induction conditions, and to reveal the key influencing factors and related genes and processes underlying AR formation by transcriptomic analysis. By better elucidating the mechanism of AR formation of *E. excelsum* *in vitro*, research on biological conservation and genetic engineering of *E. excelsum* can be promoted and advanced.

Materials And Methods

Culture of plantlets

The basic micropropagation system for *E. excelsum* that was previously established (Chen et al 2020b), was employed in this study. *In vitro* plantlets were maintained and propagated on WPM supplemented with 4.44 μM BA (Solarbio, Beijing, China) and 0.53 μM NAA (Macklin, Shanghai, China). Single shoots with more than four leaves and two nodes cut from multiple shoots were inoculated on PGR-free WPM for 30 days. During this period, AR was not induced.

All media contained 20 g/L sucrose and 0.5% (w/v) agar, and pH was adjusted to 5.8-6.0, then autoclaved at 116°C for 30 min. Culture jars (140 cm high; 90 cm diameter; 550 mL) were placed in an air-conditioned culture room at $25 \pm 2^\circ\text{C}$ with a 12-h photoperiod under $100 \mu\text{m}^{-2} \text{s}^{-1}$ fluorescent light (Philips, Tianjing, China) and 50-70% relative humidity.

Adventitious root induction

For the *in vitro* rooting treatment, 2 mm of the base of single shoots cultured on PGR-free WPM for 30 days were cut and trimmed shoots were inoculated on WPM supplemented with 0, 0.05, 0.5, and 5 μM NAA, IBA or IAA (Macklin). Shoots in the control group were inoculated on PGR/auxin-free WPM. Ten shoots were placed in each jar, and four jars were prepared for each treatment. Three replicates were performed for each treatment (n = 12 jars; 120 shoots in total).

For the *ex vitro* rooting treatment, single shoots cultured on PGR-free WPM for 30 days were removed from culture jars, and about 2 mm was trimmed from the base. Trimmed shoots were treated with 0, 1, 2,

and 3 mM NAA, IBA or IAA for 10 min, then transferred to plates (5 cm in height; 27 cm in width; 47 cm in length) for raising seedlings supplemented with vermiculite and perlite (v/v, 1:1). Trimmed shoots cultured on PGR/auxin-free WPM served as the control. Forty shoots were planted in each plate, and three replicate plates were prepared for each treatment (n = 3 plates; 120 shoots in total).

Rooting percentage as well as average root number and root length were calculated for each treatment. After one-way analysis of variance (ANOVA), treatment means were compared by Duncan's multiple range test (DMRT) in SPSS Statistics version 20.0 (IBM, New York, USA) and were considered to be significantly different from controls at $P < 0.05$.

Histological analysis

The base of shoots (0.5-1.0 cm) was collected at 0, 2, 4, 6, 8, 10 and 12 d after the optimum treatment method under *ex vitro* rooting and fixed for 24 h in formalin/acetic acid/alcohol at $25 \pm 2^\circ\text{C}$. At least 15 bases were collected for each time point. Fixed material was dehydrated in a 70-100% alcohol dehydration series followed by infiltration with molten paraffin (Mackin), and embedded in paraffin wax. Sections (8-10 μm thick) were made with a rotary microtome (KEDEE, Zhejiang, China) and stained in 0.02-0.05% toluidine blue (Mackin). Sections were viewed with a Nikon Eclipse E200 microscope (Nikon, Tokyo, Japan) and micrographs were captured using a HQimage C630 digital camera (Hengqiao, Hangzhou, China).

Determination of endogenous IAA and hydrogen peroxide (H_2O_2) content

To analyze IAA and H_2O_2 content, the same method and growth conditions were employed as for histological analysis. Material was stored at -80°C . Three biological replicates of 10 cut stem bases were harvested as 0.1 g fresh weight (FW) to assess endogenous IAA and H_2O_2 content, according to the instructions of an IAA Enzyme Linked Immunosorbent Assay kit (Dogesce, Beijing, China) (Zhang et al 2017) and Hydrogen Peroxide Assay kit (Solarbio, Beijing, China) (Wang et al 2019). After one-way ANOVA, treatment means were assessed by DMRT in SPSS Statistics version 20.0 and were considered to be significantly different from controls at $P < 0.05$.

Isolation of RNA and cDNA library construction

The same samples used to analyze IAA and H_2O_2 content were employed for RNA-seq analysis. Samples collected from 0, 2, 4, 6, 8, 10, and 12 d were marked as ER0, ER2, ER4, ER6, ER8, ER10, ER12, respectively, and stored at -80°C . The Column Plant RNA_{OUT} Extraction kit (Tiandz, Beijing, China) was used to isolate total RNA from each sample, using the methods suggested by the manufacturer. The concentration and quality of all RNA samples was examined by agarose electrophoresis on an Agilent 2100 bioanalyzer (Agilent Technologies, Palo Alto, CA, USA). Sequencing libraries were generated using the TruSeq RNA Sample Preparation Kit (Illumina, San Diego, CA, USA). Magnetic beads with oligo(dT) were used to purify mRNA, which was fragmented into short fragments (200-300 bp). Cleaved mRNA fragments were primed with a random hexamer primer for first-strand and second-strand cDNA synthesis. After purification, end

repair, and ligation to sequencing adapters, 21 cDNA libraries of three biological replicates for each treatment were prepared and sequenced using the Illumina Novaseq 6000 platform by Personal Biotechnology Co., Ltd. (Shanghai, China).

Sequencing and functional annotation

Empty reads, adapter sequences, and low-quality reads were discarded from raw reads to obtain clean reads. The *de novo* assembly of high-quality reads was performed by Trinity software (version 2.5.1, <https://github.com/trinityrnaseq/trinityrnaseq/wiki>). Assembled transcripts were aligned to NCBI non-redundant protein sequences (NR, <http://ftp.ncbi.nlm.nih.gov/blast/db/FASTA/>), Gene Ontology (GO, (<https://www.blast2go.com/>), Kyoto Encyclopedia of Genes and Genomes (KEGG, KAAS (<http://kobas.cbi.pku.edu.cn/>), evolutionary genealogy of genes: Non-supervised Orthologous Groups (eggNOG, http://eggnoG.embl.de/version_3.0), Swiss-Prot (<http://www.uniprot.org/help/uniprotkb>) and Pfam (<http://pfam.xfam.org/>) using BLASTX with a significance threshold of $E \leq 10^{-5}$.

Identification and functional annotation of differentially expressed genes (DEGs)

Gene expression level was calculated with the fragments per kilobase per transcript per million mapped reads method (FPKM). In comparisons between libraries, genes showing $|\log_2 \text{FoldChange}| > 1$ and a P value < 0.05 were identified as DEGs by DESeq software (<http://www.bioconductor.org/packages/release/bioc/html/DESeq.html>). The expression pattern of DEGs in the ER0, ER2, ER4, ER6, ER8, ER10 and ER12 libraries were analyzed by hierarchical clustering using Pheatmap software (<https://cran.r-project.org/web/packages/pheatmap/index.html>). The significantly enriched GO terms and KEGG pathways of DEGs were detected with a corrected P -value < 0.05 by the hypergeometric test method (Eden et al 2009, Mao et al 2005).

Quantitative reverse transcription-polymerase chain reaction (qRT-PCR) analysis

Ten candidate DEGs in the significant enrichment KEGG pathway were randomly chosen for qRT-PCR analysis to validate the transcriptomic data. qRT-PCR was performed with the LightCycler 480 System (Roche Diagnostics, Mannheim, Germany) using PerfectStart Green qPCR Supermix (TransGen Biotech, Beijing, China). *E. excelsum* actin was used as the internal control and the $2^{-\Delta\Delta C_t}$ method (Livak and Schmittgen 2001) was used to analyze the differential expression of candidate DEGs. Gene-specific primers are listed in Table S1. Three biological replicates and three technical replicates were performed for each candidate gene.

Results

Adventitious root formation during *in vitro* and *ex vitro* rooting

During *in vitro* rooting, compared with the control group, NAA did not induce ARs whereas IBA or IAA could. High concentrations of IBA and IAA inhibited rooting percentage (Fig. 1a), root number (Fig. 1b)

and root length (Fig. 1c). Highest rooting percentage (72.50%) was obtained by 0.5 μ M IAA 60 d after treatment. During *ex vitro* rooting, NAA, IBA and IAA significantly increased rooting percentage (Fig. 1d), root number (Fig. 1e) and root length (Fig. 1f) compared with the control group. A low concentration of IBA (1 mM) most effectively induced rooting, resulting in the highest rooting percentage (98.33%) and root length (2.72 cm) 25 d after treatment.

Ex vitro rooting induced the highest rooting percentage (98.33%) at 25 d, while highest rooting percentage during *in vitro* rooting was 72.50% at 60 d. Thus, *ex vitro* rooting induced AR from *E. excelsum* plantlets earlier (faster) than *in vitro* rooting. The samples collected from *ex vitro* rooting were used for the next analysis. Eight days after the 1 mM IBA *ex vitro* rooting treatment, AR primordia were evident, and ARs emerged from the epidermis after 10 d (Fig. 2). ARs elongated, rooting percentage was almost 100% by 25 d, and plantlet survival reached 100%.

IAA and H₂O₂ content analysis

In the 1 mM IBA treatment during *ex vitro* rooting, IAA content in stem bases increased gradually from 0 to 8 d, then dropped at 10 and 12 d. A sharp increase in IAA content was observed at 8 d (Fig. 3a). The trend of H₂O₂ content was different from that of IAA content (Fig. 3b). H₂O₂ accumulated rapidly after treatment, peaked at 2 d, then sharply decreased at 8 d. The highest content of IAA and lowest content of H₂O₂ at 8 d corresponded to the timing of AR primordia formation.

De novo assembly and sequence analysis

To identify genes involved in AR induction of *E. excelsum* plantlets during *ex vitro* rooting, 21 cDNA libraries were prepared from three repeat mRNA samples collected from 0 (ER0), 2 (ER2), 4 (ER4), 6 (ER6), 8 (ER8), 10 (ER) and 12 (ER12) d after 1 mM IBA treatment (Table 1). The total number of raw reads produced for each library ranged from 42,845,192 to 52,575,518 with Q20 > 97.48%. The sequenced raw data was submitted to the SRA at the NCBI database with the following accession numbers: SRR14278060, SRR14278059, SRR14278048, SRR14278046, SRR14278045, SRR14278044, SRR14278043, SRR14278042, SRR14278041, SRR14278040, SRR14278058, SRR14278057, SRR14278056, SRR14278055, SRR14278054, SRR14278053, SRR14278052, SRR14278051, SRR14278050, SRR14278049, and SRR14278047. After filtering, the clean reads per library ranged from 39,721,158 to 49,142,018 with the percentage of clean reads > 91.07% (Table 1). Trinity software was used to assemble clean reads and obtain transcripts and unigenes for subsequent analysis. The quality of transcripts and length distribution of unigenes are shown in Fig. S1.

The unigenes were processed in six databases to perform best hits by Blast with *E* values < 10⁻⁵, and inferred putative functions of the sequences were assigned. A total of 52,188 (40.15%) unigenes were matched to known genes in the NR database, 23,159 (17.82%) sequences to Pfam and 37,827 (29.10%) sequences in the Swiss-Prot database (Table 2). The NR database queries revealed that the annotated unigenes were assigned with a best score to sequences from the top seven species (Fig. 4): *Vitis vinifera*

(21.76%), *Theobroma cacao* (4.34%), *Coffea canephora* (4.01%), *Nelumbo nucifera* (3.88%), *Sesamum indicum* (3.13%), *Ziziphus jujuba* (2.67%) and *Manihot esculenta* (2.25%).

The annotation of GO terms revealed that 24,939 unigenes (19.19%) were assigned to biological processes, molecular functions, and cellular components (Fig. S2). Most annotated unigenes in biological processes were involved in “cellular process”, “metabolic process”, and “single-organism process”. In the cellular component category, most annotated unigenes were annotated as “cell”, “cell part” and “membrane”. In the molecular functions, most annotated unigenes were categorized as “binding”, “catalytic activity” and “transporter activity”.

A total of 22,160 unigenes (17.05%) and 33 pathways were assigned based on metabolism, genetic information processing, environmental information processing, cellular processes and organismal systems pathway (Fig. S3). On the basis of KEGG analysis, most unigenes were annotated into “carbohydrate metabolism” of metabolism, “translation” of genetic information processing, “signal transduction” of environmental information processing, “transport and catabolism” of cellular processes, and “endocrine system” of organismal system.

The possible functions of unigenes were predicted and classified by alignment to the eggNOG database. A total of 50,632 unigenes (38.95%) were distributed into 25 categories (Fig. S4). Among them, the NOG category “general function prediction only” represented the largest group, followed by “function unknown”, “signal transduction mechanisms”, and “posttranslational modification, protein turnover, chaperones”.

DEGs in response to IBA-induced *ex vitro* rooting

Hierarchical clustering was used to analyze the expression patterns of DEGs in ER0, ER2, ER4, ER6, ER8, ER10 and ER12 libraries with three biological replicates. These DEGs were divided into nine main clusters (Fig. S5). DEGs in clusters 1, 2, 3 and 4 always showed high expression in the ER0 library with different trends in the other six libraries. The remaining five clusters represented DEGs with high expression levels induced by IBA treatment. The highest number of up-regulated genes was observed in the ER2 library (7,364) and fewest in the ER8 library (5,649) (Fig. 5a). Upset plot diagram analysis showed that 4,635 unigenes maintained differential expression after IBA-induced treatment from 2 to 12 d (Fig. 5b).

GO enrichment analysis

According to GO enrichment analysis, the degree of enrichment was measured based on the rich factor (higher rich factor represents greater enrichment), the FDR value (range from 0 to 1; a score close to 0 indicates more significant enrichment) and the number of genes enriched to a GO term. The significant enrichment GO terms of DEGs showed a few differences in the six libraries (Fig. S6). In the ER2 library, the significantly enriched terms were “monooxygenase activity”, “response to auxin” and “oxidoreductase activity, acting on paired donors, with incorporation or reduction of molecular oxygen”. In the ER4 library, the significantly enriched terms were the same as the ER2 library, but the term

“response to auxin” was replaced by “photosynthesis, light reaction”. In the ER6 and ER8 libraries, “monooxygenase activity” and “photosystem” were listed as significantly enriched terms. In the ER10 library, “photosynthesis, light harvesting”, “chlorophyll binding” and “photosystem I” represented the main significantly enriched terms. In the ER12 library, the significantly enriched terms were “hydrogen peroxide metabolic process”, “hydrogen peroxide catabolic process” and “phenylpropanoid metabolic process”.

Besides “hydrogen peroxide metabolic process” and “hydrogen peroxide catabolic process”, several terms related to adversity stress were also identified in the GO enrichment analysis (Fig. 6). The terms “hydrogen peroxide metabolic process” and “hydrogen peroxide catabolic process” shared the same number and type of DEGs, most of which, including DEGs for the “response to oxidative stress” term, were up-regulated at 8 d after *ex vitro* treatment with IBA (Table S2). Most DEGs were associated with the term “response to abiotic stimulus”, followed by “response to oxidative stress” and “response to biotic stimulus”, while the fewest DEGs were associated with the term “response to hydrogen peroxide” (Fig. 6a). Most of the DEGs in the terms “response to abiotic stimulus” and “response to biotic stimulus” were up-regulated throughout the entire process of AR formation (Table S2). The terms “hydrogen peroxide metabolic process”, “hydrogen peroxide catabolic process” and “response to oxidative stress” encompassed 43 DEGs simultaneously (Fig. 6b), and these were mainly identified as genes related to cationic peroxidase and peroxidase (Table S2).

KEGG enrichment analysis

KEGG pathway enrichment analysis was performed in addition to GO enrichment analysis, and the pathways significantly enriched in each stage were similar (Fig. S7). DEGs were extremely enriched in “photosynthesis – antenna proteins”, “diterpenoid biosynthesis”, “brassinosteroid biosynthesis”, “flavone and flavanol biosynthesis” and “flavonoid biosynthesis” pathways in the ER2, ER4, ER6, ER8, ER10 and ER12 libraries. Most DEGs were enriched in “plant hormone signal transduction” and “phenylpropanoid biosynthesis” pathways.

DEGs enriched in plant hormone signal transduction pathway

KEGG pathway enrichment analysis showed that many DEGs were enriched in the “plant hormone signal transduction” pathway, and 132 up-regulated DEGs involved in auxin, cytokinin, gibberellin, abscisic acid, ethylene, brassinosteroids, jasmonic acid and salicylic acid signal transduction were identified, including genes encoding auxin-induced protein (*AUX*), auxin-responsive proteins (*SMALL AUXIN UP RNA*, *SAUR*, *Auxin/Indole-3-Acetic Acid*, *AUX/IAA*; *Indole-3-acetic acid-amido synthetase Gretchen Hagen3*, *GH3*), auxin transporter-like protein (*AUX1/LAX*), ethylene-responsive transcription factor (*ERF*), and others (Table S3). The up-regulated expression of 24 DEGs was maintained after the IBA-induced *ex vitro* treatment, mainly *SAUR50*, *SAUR32*, *SAUR36*, *IAA11*, *IAA13*, *IAA16*, *GH3.1*, *GH3.5*, *GH3.6*, and *ERF*.

A total of 42 up-regulated genes related to auxin-responsive proteins, including 13 *IAA*, 19 *SAUR* and 10 *GH3* genes, were identified in the significantly enriched pathway “plant hormone signal transduction” (Fig. 7). Most of those genes were differentially expressed in early response to IBA treatment, at 2 and 4

d. Four *IAA* and three *SAUR* genes sustained up-regulated expression after IBA-induced treatment. *IAA17* (TRINITY_DN5977_c2_g1) showed high expression with $\log_2(\text{FC}) > 4$ at ER2, ER4, ER6, ER8, and ER10 stages, and even with $\log_2(\text{FC}) > 8$ at the ER2 stage. *IAA30* (TRINITY_DN1790_c2_g1) showed high expression with $\log_2(\text{FC}) > 4$ at all stages, and even with $\log_2(\text{FC}) > 8$ at the ER2 and ER4 stages. Some DEGs were specifically differentially expressed at certain stages, such as TRINITY_DN14445_c0_g2 at ER2, TRINITY_DN58019_c0_g2 at ER10, and TRINITY_DN1958_c1_g2, TRINITY_DN25899_c0_g1, TRINITY_DN58019_c0_g1 and TRINITY_DN9289_c0_g1 at ER12. Five *GH3* genes were up-regulated at all stages, demonstrating $\log_2(\text{FC}) > 4$ for TRINITY_DN2748_c0_g1 and TRINITY_DN2800_c0_g1, and $\log_2(\text{FC}) > 8$ for TRINITY_DN5152_c0_g1.

The 12 up-regulated genes related to auxin-induced proteins, identified as *AX6B*, *AX10A*, *A10A5*, *AX15A*, *AUX22*, *AUX22D*, and *AUX28*, were sharply enriched in the “plant hormone signal transduction” pathway (Fig. 8a). Most of those genes were also differentially expressed at an early stage (2, 4 d) after IBA treatment. Among these genes, TRINITY_DN39834_c0_g1 and TRINITY_DN31248_c0_g1 were extremely highly differentially expressed with $\log_2(\text{FC}) > 8$ in the ER0 vs ER2 and ER0 vs ER4 comparisons. Four DEGs were up-regulated with $\log_2(\text{FC}) > 1$ by IBA treatment under *ex vitro* rooting in the ER0 vs ER2, ER0 vs ER4, ER0 vs ER6 and ER0 vs ER8 comparisons while TRINITY_DN5677_c0_g1 maintained up-regulated expression at all stages.

In addition, five up-regulated *LAX* genes (Fig. 8b) were significantly enriched in the “plant hormone signal transduction” pathway. Only TRINITY_DN9654_c0_g1 was up-regulated at all stages while the other four *LAX* genes were up-regulated at ER10 and ER12, except for TRINITY_DN380_c4_g1, which was up-regulated at ER6.

QRT-PCR analysis of gene expression

To further validate the results from the RNA-seq data, 10 candidate DEGs were selected for qRT-PCR analysis of *E. excelsum* samples that were collected 0, 2, 4, 6, 8, 10 and 12 d after 1 mM IBA treatment during *ex vitro* rooting. In the seven time points, the expression trend of the unigenes from qRT-PCR and RNA-seq analysis were largely consistent (Fig. 9). These results demonstrate that the transcriptome data accurately reflects the *ex vitro* response of IBA-induced AR formation of *E. excelsum* plantlets.

Discussion

AR development is a vital step in plant vegetative propagation, such as *in vitro* propagation and cuttings. Rooting recalcitrance is a critical factor limiting the application and further development of vegetative propagation (Diaz-Sala 2020, Stevens et al 2018). IBA is the most frequently used plant hormone for clonal propagation in horticulture and forestry. Although IAA is a primarily native auxin in plants, IBA is more stable and effective in promoting ARs (Ludwig-Muller et al 2005, Quan et al 2017, Rout 2006). It is necessary to screen PGRs to find the optimal species-concentration ratio for AR induction during *in vitro* culture. In this study, IBA and IAA treatment significantly promote AR formation of *E. excelsum*, especially

during *ex vitro* rooting. Furthermore, *ex vitro* rooting was more suitable for *E. excelsum* plantlets, with a higher rooting percentage and earlier rooting than *in vitro* rooting. *Ex vitro* rooting of shoots has also been applied to many difficult-to-root woody plant species, such as pistachio (Benmahioul et al 2012), *Dalbergia sissoo* Roxb. (Vibha et al 2014) and *Bauhinia racemosa* Lam (Sharma et al 2017). In general, the chances of root damage during transplantation to substrates are less during *ex vitro* rooting, and plantlets tend to be more vigorous, allowing them to cope with environmental stresses during hardening (Arya et al 2003, Vengadesan and Pijut 2009). Thus, *ex vitro* rooting is an obvious choice for AR induction during the micropropagation of woody species with further improvement in the choice of PGRs, substrates and other factors.

E. excelsum plantlets experienced a radical environmental change from *in vitro* aseptic conditions to open *ex vitro* rooting conditions, which may constitute an abiotic stress. In the annotation and enrichment analysis of GO terms, we identified multiple DEGs involved in H₂O₂-related biological activities, oxidative stress, abiotic and biotic stimulus. AR formation is also a stress response of plants under adversity stress, and plays a key function in the adaptation of plants to abiotic and biotic stresses (Bellini et al 2014, Steffens and Rasmussen 2016). The external environmental may stimulate oxidative damage and increase the production of reactive oxygen species in plants (You and Chan 2015). H₂O₂ is viewed mainly as a type of reactive oxygen species and a signaling messenger of many biological processes in plants, such as fruit growth and development (Khandaker et al 2012), leaf senescence (Lin et al 2019), stomatal closure (Zhang et al 2019a), and root growth (Xiong et al 2015). H₂O₂ and IBA may also act synergistically to regulate adventitious rooting, dependent on the auxin pathway, in marigold explants (Liao et al 2011). The exogenous application of H₂O₂ to cucumber plants significantly increased the emergence of ARs (Li et al 2016b). In this study, the wide fluctuation of endogenous IAA and H₂O₂ content in *E. excelsum* plantlets were observed at the stage of root primordia formation. And most DEGs involved in significantly enriched pathway of “plant hormone signal transduction” were up-regulated at the stage corresponded to the timing of H₂O₂ accumulation. Those results indicate that adversity stress may have a positive effect on AR induction of *E. excelsum* plantlets under the synergistic action of H₂O₂ and PGRs. The synergistic action of H₂O₂ and PGRs on AR induction from *E. excelsum* plantlets will be revealed by additional research.

AR formation involves a series of responses by genes, proteins and metabolites. Multiple biological activities and pathways have specific roles during AR development (de Almeida et al 2020, Wei et al 2014). In mungbean seedlings, KEGG pathway enrichment during transcriptomic analysis showed that ribosome biogenesis, plant hormone signal transduction, pentose and glucuronate interconversions, photosynthesis, phenylpropanoid biosynthesis, sesquiterpenoid and flavonoid biosynthesis, and phenylalanine metabolism were the pathways most highly regulated by IBA-induced AR formation, indicating their potential contribution to adventitious rooting (Li et al 2016a). For apple rootstocks, the most heavily enriched KEGG pathways involved in AR formation were metabolic, biosynthesis of secondary metabolites, plant hormone signal transduction, phenylpropanoid biosynthesis and phenylalanine metabolism pathways, etc. (Li et al 2018). In sugarcane shoots, DEGs associated with

plant hormone signaling, flavonoid and phenylpropanoid biosynthesis, cell cycle, and cell wall modification, and transcription factors were involved in AR formation (Li et al 2020). During AR development of *E. excelsum*, we found that more DEGs were enriched in “plant hormone signal transduction” and “phenylpropanoid biosynthesis” pathways, similar to a number of previous studies. Therefore, we conclude that these two pathways have a vital influence on AR formation in *E. excelsum* plants.

IAA is the most abundant natural auxin, and endogenous IAA is closely related to the development of ARs in plants. The conversion of exogenous hormones to endogenous auxin and the synthesis of auxin are key factors regulating AR development (Olatunji et al 2017). Tissue that produces ARs requires high levels of auxin, and the enrichment of high concentrations of auxin depends on polar auxin transport (Ahkami et al 2013, Garrido et al 2002). Thus, genes related to the synthesis, signaling and polar transport of auxin, like *AUX*, *LAX*, and *PIN*, are closely related to plant adventitious rooting (Druege et al 2016). For example, auxin influx carriers *MiAUX3* and *MiAUX4* might play important roles during AR formation in mango cotyledon segments, and the expression levels of *MiAUX3* and *MiAUX4* resulted in a significant promotive effect of IBA on adventitious rooting (Li et al 2012). Papaya plantlets not exposed to IBA could not form ARs and displayed a low expression of all auxin transporter genes in stem base tissues whereas IBA-treated plants were able to produce ARs and showed significantly increased expression of most auxin transporter genes, especially *CpLAX3* and *CpPIN2* (Estrella-Maldonado et al 2016). In *E. excelsum*, DEGs for *AUX* and *LAX*, which were significantly enriched in plant hormone signal transduction, showed a high fold change during AR development. This implies that the expression patterns of those genes were linked to AR induction from *E. excelsum* plantlets.

AUX/IAA protein is an early auxin response protein that always participates in the auxin signaling pathway by interacting with auxin response factor (ARF) protein or other genes (Salehin et al 2015). During AR formation in petunia cuttings, the expression of genes of the *Aux/IAA* family showed strong temporal variation, supporting their important role in the induction and transition to subsequent root formation phases (Druege et al 2014). The auxin receptor (TRANSPORT INHIBITOR1) TIR1 homolog gene, *PagFBL1*, interacted strongly with both *PagIAA28.1* and *PagIAA28.2* in the presence of NAA to regulate AR induction in poplar stem segments (Shu et al 2019). In *Arabidopsis thaliana*, *Aux/IAA* proteins, *IAA6*, *IAA9*, and *IAA17*, interacted with ARF6 and/or ARF8 and likely repressed their activity in AR development, and complexed with TIR1 and (AUXIN-SIGNALING F-BOX) AFB2 to form specific sensing to modulate jasmonic acid homeostasis and control AR initiation (Lakehal et al 2019). In this study, 13 *IAA* genes were significantly enriched in the plant hormone signal transduction pathway, suggesting a significant relationship between *AUX/IAA* and AR formation in *E. excelsum*. The mechanism and interaction with other *IAA* genes would need to be revealed in future research.

SAUR, the largest family of early auxin response genes in plants, mediate the regulation of several aspects of plant growth and development (Ren and Gray 2015). *SAUR* proteins showed positive or negative effects on primary, lateral and adventitious root development. In *A. thaliana*, plants overexpressing *SAUR41* exhibited increased primary root growth and a higher number of lateral roots

(Kong et al 2013). *AtSAUR15* acts downstream of the auxin response factors ARF6,8 and ARF7,19 to regulate auxin signaling-mediated lateral root and AR formation, and plants overexpressing *AtSAUR15* exhibit more lateral roots and ARs (Yin et al 2020). In contrast to *AtSAUR41* and *AtSAUR15*, overexpression of *OsSAUR39* in rice resulted in reduced root elongation and lateral root development (Kant et al 2009). SAUR proteins may display a species- or type-dependent positive function in AR formation. In *E. excelsum*, three *SAUR* genes maintained up-regulated expression after IBA-induced treatment, indicating a close association with AR formation.

We also found several highly up-regulated *GH3* genes at all stages of AR formation in *E. excelsum*. GH3 proteins are also an early auxin response protein, play a crucial role in conjugating IAA to amino acids, and are critical in maintaining auxin homeostasis (Brunoni et al 2020). Three *GH3* genes, *GH3.3*, *GH3.5*, and *GH3.6*, were required for fine-tuning AR initiation in *A. thaliana* hypocotyls (Gutierrez et al 2012). In cucumber hypocotyls, salicylic acid plays an inducible role in AR formation through competitive inhibition of the auxin conjugation enzyme *CsGH3.5*, and salicylic acid-induced IAA accumulation was also associated with the enhanced expression of *CsGH3.5* (Dong et al 2020). In apple plants, overexpression of *MsGH3.5* significantly reduced the content of free IAA and increased the content of some IAA-amino acid conjugates, and *MsGH3.5*-overexpressing lines produced fewer ARs than the control (Zhao et al 2020). Those results demonstrated that GH3 proteins were intricately involved in AR development, but did not only perform a positive role.

Conclusion

Here, we confirmed that *ex vitro* rooting was an obvious choice for AR formation during the micropropagation of *E. excelsum* plantlets. DEGs enriched in the pathway of plant hormone signal transduction played a crucial role in AR formation. H₂O₂ produced by environmental stimulation might be related to AR induction in *E. excelsum ex vitro* by the synergistic action with IBA, ultimately regulating the level of endogenous IAA. The knowledge gained from this study will help researchers understand the molecular traits of IBA-based regulation of adventitious rooting of *E. excelsum* plantlets. These results are important for research and commercial applications aimed at overcoming rooting recalcitrance in plant species of economic value, in difficult-to-root woody plants, or in rare or endangered plants.

Abbreviations

AR	Adventitious root
AUX	Auxin-induced protein
AUX/IAA	Auxin/Indole-3-Acetic Acid
AUX/LAX	Auxin transporter-like protein
ARF	Auxin response factor
BA	6-Benzyladenine
cDNA	Complementary deoxyribonucleic acid
DEG	Differentially expressed gene
eggNOG	Evolutionary genealogy of genes: Non-supervised Orthologous Groups
ERF	Ethylene-responsive transcription factor
FC	Fold change
FPKM	Fragments per kilobases per million mapped reads
FW	Fesh weight
GH3	Indole-3-acetic acid-amido synthetase Gretchen Hagen3
GO	Gene ontology
IAA	Indole-3-acetic acid
IBA	Indole-3-butyric acid
JA	Jasmonic acid
KEGG	Kyoto Encyclopedia of Genes and Genomes
NAA	α -Naphthaleneacetic acid
NCBI	National Center for Biotechnology Information
NR	NCBI non-redundant protein sequences
PCR	Polymerase chain reaction
QRT-PCR	Quantitative reverse transcription-polymerase chain reaction
RNA	Ribonucleic acid
RNA-seq	High-throughput RNA-sequencing
SA	Salicylic acid
SAUR	SMALL AUXIN UP RNA
WPM	Woody plant medium

Declarations

Ethics approval and consent to participate

Specific permission was not required for plant collection at the mentioned locations.

Consent for publication

Not applicable.

Data and Materials Availability

All data generated or analyzed during this study are included in this published article and its supplementary information files. The RNA-seq data has been deposited in the Sequence Read Archives Database (<https://www.ncbi.nlm.nih.gov/sra/>) under accession number PRJNA723111 (<http://www.ncbi.nlm.nih.gov/bioproject/723111>).

Conflicts of interest

The authors declare that they have no competing interests.

Funding

This work was supported by the National Key Research Plan of China (Grant Number: 2016YFC0503104) and Guangdong Province Science and Technology Program (Number: 2015B020231008).

Acknowledgement

We thank Personal Biotechnology Co., Ltd. for their skillful support of RNA-sequencing.

Authors' contributions

XHZ, YL, KLW, FL, JATdS, GHM and SJZ designed the experiment and provided guidance on the study. YPX and SYC prepared samples for AR induction and RNA-seq analysis. XHC, TZ, BYG and MYN performed the statistical analysis on the determination of IAA and H₂O₂ content, and RNA-seq data. ZPW, YYY, XCY and JHP participated in the experiment of AR induction and anatomical analysis. YPX, JATdS and SYC were involved in statistical analyses and co-wrote the manuscript. All authors wrote, read and approved the manuscript.

References

1. Ahkami AH, Melzer M, Ghaffari MR, Pollmann S, Javid MG, Shahinnia F, Hajirezaei MR, Druege U (2013) Distribution of indole-3-acetic acid in *Petunia hybrida* shoot tip cuttings and relationship between auxin transport, carbohydrate metabolism and adventitious root formation. *Planta* 238:499-517. <http://dx.doi.org/10.1007/s00425-013-1907-z>

2. Arya V, Shekhawat NS, Singh RP (2003) Micropropagation of *Leptadenia reticulata* - A medicinal plant. *In Vitro Cell Dev Biol—Plant* 39:180-185. <http://dx.doi.org/10.1079/lvp2002394>
3. Barlow PW. 1986. Adventitious roots of whole plants: their forms, functions, and evolution. In *New Root Formation in Plants and Cuttings* Ed. M.B. Jackson. Springer Netherlands, Dordrecht, 67-110.
4. Barpete S, Khawar KM, Özcan S (2014) Differential competence for *in vitro* adventitious rooting of grass pea (*Lathyrus sativus* L.). *Plant Cell Tiss Organ Cult* 119:39-50. <http://dx.doi.org/10.1007/s11240-014-0512-6>
5. Barstow M (2020) *Euryodendron excelsum* (amended version of 2017 assessment). The IUCN Red List of Threatened Species 2020: <https://dx.doi.org/10.2305/IUCN.UK.2020-2303.RLTS.T32348A177362929.en>.
6. Bellini C, Pacurar DI, Perrone I (2014) Adventitious roots and lateral roots: similarities and differences. *Annu Rev Plant Biol* 65:639-667. <http://dx.doi.org/10.1146/annurev-arplant-050213-035645>
7. Benmahiou B, Dorion N, Kaid-Harche M, Daguin F (2012) Micropropagation and *ex vitro* rooting of pistachio (*Pistacia vera* L.). *Plant Cell Tiss Organ Cult* 108:353-358. <http://dx.doi.org/10.1007/s11240-011-0040-6>
8. Bhardwaj AK, Singh B, Kaur K, Roshan P, Sharma A, Dolker D, Naryal A, Saxena S, Pati PK, Chaurasia OP (2018) *In vitro* propagation, clonal fidelity and phytochemical analysis of *Rhodiola imbricata* Edgew: a rare trans-Himalayan medicinal plant. *Plant Cell Tiss Organ Cult* 135:499-513. <http://dx.doi.org/10.1007/s11240-018-1482-x>
9. Brunoni F, Collani S, Casanova-Saez R, Simura J, Karady M, Schmid M, Ljung K, Bellini C (2020) Conifers exhibit a characteristic inactivation of auxin to maintain tissue homeostasis. *New Phytol* 226:1753-1765. <http://dx.doi.org/10.1111/nph.16463>
10. Cardoso JC, Teixeira da Silva JA (2013) Micropropagation of *Zeyheria montana* Mart. (Bignoniaceae), an endangered endemic medicinal species from the Brazilian cerrado biome. *In Vitro Cell Dev Biol—Plant* 49:710-716. <http://dx.doi.org/10.1007/s11627-013-9558-0>
11. Chang HT (1963) *Euryodendron*, a new genus of Theaceae. *Acta Sci Natur Univ Sunyatseni*:126-130.
12. Chen QJ, Deng BH, Gao J, Zhao ZY, Chen ZL, Song SR, Wang L, Zhao LP, Xu WP, Zhang CX, Ma C, Wang SP (2020a) A miRNA-encoded small peptide, vvi-miPEP171d1, regulates adventitious root formation. *Plant Physiol* 183:656-670. <http://dx.doi.org/10.1104/pp.20.00197>
13. Chen SY, Xiong YP, Wu T, Wu KL, Teixeira da Silva JA, Xiong YH, Zeng SJ, Ma GH (2020b) Axillary shoot proliferation and plant regeneration in *Euryodendron excelsum* H. T. Chang, a critically endangered species endemic to China. *Sci Rep* 10:14402. <http://dx.doi.org/10.1038/s41598-020-71360-9>
14. de Almeida MR, Schwambach J, Silveira V, Heringer AS, Fett JP, Fett-Neto AG (2020) Proteomic profiles during adventitious rooting of *Eucalyptus* species relevant to the cellulose industry. *New Forest* 51:213-241. <http://dx.doi.org/10.1007/s11056-019-09728-7>

15. Diaz-Sala C (2020) A perspective on adventitious root formation in tree species. *Plants* (Basel) 9(12):1789. <http://dx.doi.org/10.3390/plants9121789>
16. Dong CJ, Liu XY, Xie LL, Wang LL, Shang QM (2020) Salicylic acid regulates adventitious root formation *via* competitive inhibition of the auxin conjugation enzyme CsGH3.5 in cucumber hypocotyls. *Planta* 252:75. <http://dx.doi.org/10.1007/s00425-020-03467-2>
17. Druege U, Franken P, Hajirezaei MR (2016) Plant hormone homeostasis, signaling, and function during adventitious root formation in cuttings. *Front Plant Sci* 7:381. <http://dx.doi.org/10.3389/fpls.2016.00381>
18. Druege U, Franken P, Lischewski S, Ahkami AH, Zerche S, Hause B, Hajirezaei MR (2014) Transcriptomic analysis reveals ethylene as stimulator and auxin as regulator of adventitious root formation in petunia cuttings. *Front Plant Sci* 5:494. <http://dx.doi.org/10.3389/fpls.2014.00494>
19. Eden E, Navon R, Steinfeld I, Lipson D, Yakhini Z (2009) GOrilla: a tool for discovery and visualization of enriched GO terms in ranked gene lists. *BMC Bioinformatics* 10:48. <http://dx.doi.org/10.1186/1471-2105-10-48>
20. Estrella-Maldonado H, Ortíz GF, León ACC, Zapata LCR, May CT, Gil FEY, Pool FB, Espín FMI, Santamaría JM (2016) The papaya *CpAUX1/LAX* and *CpPIN* genes: structure, phylogeny and expression analysis related to root formation on *in vitro* plantlets. *Plant Cell Tiss Organ Cult* 126:187-204. <http://dx.doi.org/10.1007/s11240-016-0989-2>
21. Fattorini L, Veloccia A, Della Rovere F, D'Angeli S, Falasca G, Altamura MM (2017) Indole-3-butyric acid promotes adventitious rooting in *Arabidopsis thaliana* thin cell layers by conversion into indole-3-acetic acid and stimulation of anthranilate synthase activity. *BMC Plant Biol* 17:121. <http://dx.doi.org/10.1186/s12870-017-1071-x>
22. Garrido G, Guerrero JR, Cano EA, Acosta M, Sánchez-Bravo J (2002) Origin and basipetal transport of the IAA responsible for rooting of carnation cuttings. *Physiol Plant* 114(2):303-312. <http://dx.doi.org/10.1034/j.1399-3054.2002.1140217.x>
23. Guo YX, Zhao YY, Zhang M, Zhang LY (2019) Development of a novel *in vitro* rooting culture system for the micropropagation of highbush blueberry (*Vaccinium corymbosum*) seedlings. *Plant Cell Tiss Organ Cult* 139:615-620. <http://dx.doi.org/10.1007/s11240-019-01702-7>
24. Gutierrez L, Mongelard G, Floková K, Păcurar DI, Novák O, Staswick P, Kowalczyk M, Păcurar M, Demailly H, Geiss G, Bellini C (2012) Auxin controls *Arabidopsis* adventitious root initiation by regulating jasmonic acid homeostasis. *Plant Cell* 24:2515-2527. <http://dx.doi.org/10.1105/tpc.112.099119>
25. Ilczuk A, Jacygrad E (2016) *In vitro* propagation and assessment of genetic stability of acclimated plantlets of *Cornus alba* L. using RAPD and ISSR markers. *In Vitro Cell Dev Biol—Plant* 52:379-390. <http://dx.doi.org/10.1007/s11627-016-9781-6>
26. Kant S, Bi YM, Zhu T, Rothstein SJ (2009) *SAUR39*, a small auxin-up RNA gene, acts as a negative regulator of auxin synthesis and transport in rice. *Plant Physiol* 151:691-701. <http://dx.doi.org/10.1104/pp.109.143875>

27. Khandaker MM, Boyce AN, Osman N (2012) The influence of hydrogen peroxide on the growth, development and quality of wax apple (*Syzygium samarangense*, [Blume] Merrill & L.M. Perry var. *jambu madu*) fruits. *Plant Physiol Biochem* 53:101-110.
<http://dx.doi.org/10.1016/j.plaphy.2012.01.016>
28. Khater N, Benbouza H (2019) Preservation of *Juniperus thurifera* L.: a rare endangered species in Algeria through *in vitro* regeneration. *J For Res* 30:77-86. <http://dx.doi.org/10.1007/s11676-018-0628-3>
29. Kong YY, Zhu YB, Gao C, She WJ, Lin WQ, Chen Y, Han N, Bian HW, Zhu MY, Wang JH (2013) Tissue-specific expression of *SMALL AUXIN UP RNA41* differentially regulates cell expansion and root meristem patterning in *Arabidopsis*. *Plant Cell Physiol* 54:609-621.
<http://dx.doi.org/10.1093/pcp/pct028>
30. Lakehal A, Bellini C (2019) Control of adventitious root formation: insights into synergistic and antagonistic hormonal interactions. *Physiol Plant* 165:90-100. <http://dx.doi.org/10.1111/ppl.12823>
31. Lakehal A, Chaabouni S, Cavel E, Le Hir R, Ranjan A, Raneshan Z, Novák O, Păcurar DI, Perrone I, Jobert F, Gutierrez L, Bakò L, Bellini C (2019) A molecular framework for the control of adventitious rooting by TIR1/AFB2-Aux/IAA-dependent auxin signaling in *Arabidopsis*. *Mol Plant* 12:1499-1514.
<http://dx.doi.org/10.1016/j.molp.2019.09.001>
32. Lerin J, Ribeiro YRD, de Oliveira TD, Silveira V, Santa-Catarina C (2021) Histomorphology and proteomics during rooting of *in vitro* shoots in *Cariniana legalis* (Lecythidaceae), a difficult-to-root endangered species from the Brazilian Atlantic Forest. *Plant Cell Tiss Organ Cult* 144:325-344.
<http://dx.doi.org/10.1007/s11240-020-01955-7>
33. Li AM, Lakshmanan P, He WZ, Tan HW, Liu LM, Liu HJ, Liu JX, Huang DL, Chen ZL (2020) Transcriptome profiling provides molecular insights into auxin-induced adventitious root formation in sugarcane (*Saccharum* spp. interspecific hybrids) microshoots. *Plants* 9(8):931.
<http://dx.doi.org/10.3390/plants9080931>
34. Li K, Liang YQ, Xing LB, Mao JP, Liu Z, Dong F, Meng Y, Han MY, Zhao CP, Bao L, Zhang D (2018) Transcriptome analysis reveals multiple hormones, wounding and sugar signaling pathways mediate adventitious root formation in apple rootstock. *Int J Mol Sci* 19(8):2201.
<http://dx.doi.org/10.3390/ijms19082201>
35. Li SW, Shi RF, Leng Y, Zhou Y (2016a) Transcriptomic analysis reveals the gene expression profile that specifically responds to IBA during adventitious rooting in mung bean seedlings. *BMC Genomics* 17:43. <http://dx.doi.org/10.1186/s12864-016-2372-4>
36. Li XP, Xu QQ, Liao WB, Ma ZJ, Xu XT, Wang M, Ren PJ, Niu LJ, Jin X, Zhu YC (2016b) Hydrogen peroxide is involved in abscisic acid-induced adventitious rooting in cucumber (*Cucumis sativus* L.) under drought stress. *J Plant Biol* 59:536-548. <http://dx.doi.org/10.1007/s12374-016-0036-1>
37. Li YH, Zhang HN, Wu QS, Muday GK (2017) Transcriptional sequencing and analysis of major genes involved in the adventitious root formation of mango cotyledon segments. *Planta* 245:1193-1213.
<http://dx.doi.org/10.1007/s00425-017-2677-9>

38. Li YH, Zou MH, Feng BH, Huang X, Zhang Z, Sun GM (2012) Molecular cloning and characterization of the genes encoding an auxin efflux carrier and the auxin influx carriers associated with the adventitious root formation in mango (*Mangifera indica* L.) cotyledon segments. *Plant Physiol Biochem* 55:33-42. <http://dx.doi.org/10.1016/j.plaphy.2012.03.012>
39. Liao WB, Huang GB, Yu JH, Zhang ML, Shi XL (2011) Nitric oxide and hydrogen peroxide are involved in indole-3-butyric acid-induced adventitious root development in marigold. *J Hortic Sci Biotech* 86:159-165. <http://dx.doi.org/10.1080/14620316.2011.11512742>
40. Lin WF, Huang DM, Shi XM, Deng B, Ren YJ, Lin WX, Miao Y (2019) H₂O₂ as a feedback signal on dual-located WHIRLY1 associates with leaf senescence in *Arabidopsis*. *Cells* 8(12):1585. <http://dx.doi.org/10.3390/cells8121585>
41. Livak KJ, Schmittgen TD (2001) Analysis of relative gene expression data using real-time quantitative PCR and the 2^{-ΔΔCT} method. *Methods* 25:402-408. <http://dx.doi.org/10.1006/meth.2001.1262>
42. Lloyd G, McCown B (1980) Commercially feasible micropropagation of mountain laurel, *Kalmia latifolia*, by use of shoot-tip culture. *Proc Int Plant Prop Soc* 30:421–427.
43. Lozzi A, Abdelwahd R, Mentag R, Abousalim A (2019) Development of a new culture medium and efficient protocol for *in vitro* micropropagation of *Ceratonia siliqua* L. *In Vitro Cell Dev Biol—Plant* 55:615-624. <http://dx.doi.org/10.1007/s11627-019-09990-6>
44. Ludwig-Müller J, Vertocnik A, Town CD (2005) Analysis of indole-3-butyric acid-induced adventitious root formation on *Arabidopsis* stem segments. *J Exp Bot* 56:2095-2105. <http://dx.doi.org/10.1093/jxb/eri208>
45. Mao XZ, Cai T, Olyarchuk JG, Wei LP (2005) Automated genome annotation and pathway identification using the KEGG Orthology (KO) as a controlled vocabulary. *Bioinformatics* 21:3787-3793. <http://dx.doi.org/10.1093/bioinformatics/bti430>
46. Nourissier S, Monteuis O (2008) *In vitro* rooting of two *Eucalyptus urophylla* X *Eucalyptus grandis* mature clones. *In Vitro Cell Dev Biol—Plant* 44:263-272. <http://dx.doi.org/10.1007/s11627-008-9109-2>
47. Olatunji D, Geelen D, Verstraeten I (2017) Control of endogenous auxin levels in plant root development. *Int J Mol Sci* 18(12):2587. <http://dx.doi.org/10.3390/ijms18122587>
48. Qi XH, Li QQ, Shen JT, Qian CL, Xu XW, Xu Q, Chen XH (2020) Sugar enhances waterlogging-induced adventitious root formation in cucumber by promoting auxin transport and signalling. *Plant Cell and Environ* 43:1545-1557. <http://dx.doi.org/10.1111/pce.13738>
49. Quan JE, Meng S, Guo EH, Zhang S, Zhao Z, Yang XT (2017) *De novo* sequencing and comparative transcriptome analysis of adventitious root development induced by exogenous indole-3-butyric acid in cuttings of tetraploid black locust. *BMC Genomics* 18:179. <http://dx.doi.org/10.1186/s12864-017-3554-4>
50. Rameshkumar R, Largia MJV, Satish L, Shilpha J, Ramesh M (2017) *In vitro* mass propagation and conservation of *Nilgirianthus ciliatus* through nodal explants: A globally endangered, high trade

- medicinal plant of Western Ghats. *Plant Biosyst* 151:204-211.
<http://dx.doi.org/10.1080/11263504.2016.1149120>
51. Ren H, Gray WM (2015) SAUR proteins as effectors of hormonal and environmental signals in plant growth. *Mol Plant* 8:1153-1164. <http://dx.doi.org/10.1016/j.molp.2015.05.003>
 52. Revathi J, Manokari M, Shekhawat MS (2018) Optimization of factors affecting *in vitro* regeneration, flowering, *ex vitro* rooting and foliar micromorphological studies of *Oldenlandia corymbosa* L.: a multipotent herb. *Plant Cell Tiss Organ Cult* 134:1-13. <http://dx.doi.org/10.1007/s11240-018-1395-8>
 53. Rout GR (2006) Effect of auxins on adventitious root development from single node cuttings of *Camellia sinensis* (L.) Kuntze and associated biochemical changes. *Plant Growth Regul* 48:111-117. <http://dx.doi.org/10.1007/s10725-005-5665-1>
 54. Salehin M, Bagchi R, Estelle M (2015) SCF^{TIR1/AFB}-Based auxin perception: mechanism and role in plant growth and development. *Plant Cell* 27:9-19. <http://dx.doi.org/10.1105/tpc.114.133744>
 55. Sharma U, Kataria V, Shekhawat NS (2017) *In vitro* propagation, *ex vitro* rooting and leaf micromorphology of *Bauhinia racemosa* Lam.: a leguminous tree with medicinal values. *Physiol Mol Biol Plants* 23:969-977. <http://dx.doi.org/10.1007/s12298-017-0459-2>
 56. Shekhawat MS, Manokari M (2016) *In vitro* propagation, micromorphological studies and *ex vitro* rooting of cannon ball tree (*Couroupita guianensis* Aubl.): a multipurpose threatened species. *Physiol Mol Biol Plants* 22:131-142. <http://dx.doi.org/10.1007/s12298-015-0335-x>
 57. Shen SK, Ma HY, Wang YH, Wang BY, Shen GZ (2008) The structure and dynamics of natural populations of the endangered plant *Euryodendron excelsum* H. T. Chang. *Acta Ecol Sin* 28:2404-2412. doi:CNKI:SUN:STXB.0.2008-05-058.
 58. Shen SK, Wang YH, Wang BY, Ma HY, Shen GZ, Han ZW (2009) Distribution, stand characteristics and habitat of a critically endangered plant *Euryodendron excelsum* H. T. Chang (Theaceae): implications for conservation. *Plant Spec Biol* 24:133-138. <http://dx.doi.org/10.1111/j.1442-1984.2009.00248.x>
 59. Shu WB, Zhou HJ, Jiang C, Zhao ST, Wang LQ, Li QZ, Yang ZQ, Groover A, Lu MZ (2019) The auxin receptor TIR1 homolog (PagFBL 1) regulates adventitious rooting through interactions with Aux/IAA28 in *Populus*. *Plant Biotechnol J* 17:338-349. <http://dx.doi.org/10.1111/pbi.12980>
 60. Steffens B, Rasmussen A (2016) The physiology of adventitious roots. *Plant Physiol* 170:603-617. <http://dx.doi.org/10.1104/pp.15.01360>
 61. Stevens ME, Woeste KE, Pijut PM (2018) Localized gene expression changes during adventitious root formation in black walnut (*Juglans nigra* L.). *Tree Physiol* 38:877-894. <http://dx.doi.org/10.1093/treephys/tpx175>
 62. Timofeeva SN, Elkonin LA, Tyrnov VS (2014) Micropropagation of *Laburnum anagyroides* Medic. through axillary shoot regeneration. *In Vitro Cell Dev Biol—Plant* 50:561-567. <http://dx.doi.org/10.1007/s11627-014-9618-0>
 63. Vengadesan G, Pijut PM (2009) *In vitro* propagation of northern red oak (*Quercus rubra* L.). *In Vitro Cell Dev Biol—Plant* 45:474-482. <http://dx.doi.org/10.1007/s11627-008-9182-6>

64. Verstraeten I, Geelen D (2015) Adventitious rooting and browning are differentially controlled by auxin in rooting-recalcitrant *Elegia capensis* (Burm. f.) Schelpe. J Plant Growth Regul 34:475-484. <http://dx.doi.org/10.1007/s00344-015-9482-0>
65. Vibha JB, Shekhawat NS, Mehandru P, Dinesh R (2014) Rapid multiplication of *Dalbergia sissoo* Roxb.: a timber yielding tree legume through axillary shoot proliferation and *ex vitro* rooting. Physiol Mol Biol Plants 20:81-87. <http://dx.doi.org/10.1007/s12298-013-0213-3>
66. Wang YH, Min TL, Hu XL, Cao LM, He H (2002) The ecological and reproduction characteristics of *Euryodendron excelsum*, a critically endangered plant from Theaceae. Acta Bot Yunnanica 24:725-732. doi:CNKI:SUN:YOKE.0.2002-06-008
67. Wang YN, Liang CZ, Meng ZG, Li YY, Abid MA, Askari M, Wang PL, Wang Y, Sun GQ, Cai YP, Chen SY, Lina Y, Zhang R, Guo SD (2019) Leveraging *Atriplex hortensis* choline monooxygenase to improve chilling tolerance in cotton. Environ Exp Bot 162:364-373. <http://dx.doi.org/10.1016/j.envexpbot.2019.03.012>
68. Wei K, Wang LY, Wu LY, Zhang CC, Li HL, Tan LQ, Cao HL, Cheng H (2014) Transcriptome analysis of indole-3-butyric acid-induced adventitious root formation in nodal cuttings of *Camellia sinensis* (L.). PLoS ONE 9(9):e107201. <http://dx.doi.org/10.1371/journal.pone.0107201>
69. Xiong J, Yang YJ, Fu GF, Tao LX (2015) Novel roles of hydrogen peroxide (H₂O₂) in regulating pectin synthesis and demethylesterification in the cell wall of rice (*Oryza sativa*) root tips. New Phytol 206:118-126. <http://dx.doi.org/10.1111/nph.13285>
70. Yan HB, Liang CX, Yang LT, Li YR (2010) *In vitro* and *ex vitro* rooting of *Siratia grosvenorii*, a traditional medicinal plant. Acta Physiol Plant 32:115-120. <http://dx.doi.org/10.1007/s11738-009-0386-0>
71. Ye HG, Wang FG, Zhou LX, Ye YS, Huang S (2002) *Euryodendron excelsum*, an endangered plant in Theaceae. Chin J Bot 4:3. doi:CNKI:SUN:ZWZA.0.2002-04-001
72. Yin HJ, Li MZ, Lv MH, Hepworth SR, Li DD, Ma CF, Li J, Wang SM (2020) *SAUR15* promotes lateral and adventitious root development via activating H⁺-ATPases and auxin biosynthesis. Plant Physiol 184:837-851. <http://dx.doi.org/10.1104/pp.19.01250>
73. You J, Chan ZL (2015) ROS regulation during abiotic stress responses in crop plants. Front Plant Sci 6:1092. <http://dx.doi.org/10.3389/fpls.2015.01092>
74. Zhang CX, Feng BH, Chen TT, Zhang XF, Tao LX, Fu GF (2017) Sugars, antioxidant enzymes and IAA mediate salicylic acid to prevent rice spikelet degeneration caused by heat stress. Plant Growth Regul 83:313-323. <http://dx.doi.org/10.1007/s10725-017-0296-x>
75. Zhang LS, Shi X, Zhang YT, Wang JJ, Yang JW, Ishida T, Jiang WQ, Han XY, Kang JK, Wang XN, Pan LX, Lv S, Cao B, Zhang YH, Wu JB, Han HB, Hu ZB, Cui LJ, Sawa S, He JM, Wang GD (2019a) CLE9 peptide-induced stomatal closure is mediated by abscisic acid, hydrogen peroxide, and nitric oxide in *Arabidopsis thaliana*. Plant Cell Environ 42:1033-1044. <http://dx.doi.org/10.1111/pce.13475>
76. Zhang Y, Xiao ZA, Zhan C, Liu MF, Xia WX, Wang N (2019b) Comprehensive analysis of dynamic gene expression and investigation of the roles of hydrogen peroxide during adventitious rooting in

77. Zhao D, Wang YT, Feng C, Wei Y, Peng X, Guo X, Guo XW, Zhai ZF, Li J, Shen XS, Li TH (2020) Overexpression of *MsGH3.5* inhibits shoot and root development through the auxin and cytokinin pathways in apple plants. Plant J 103:166-183. <http://dx.doi.org/10.1111/tpj.14717>

Tables

Due to technical limitations, tables are only available as a download in the Supplemental Files section.

Figures

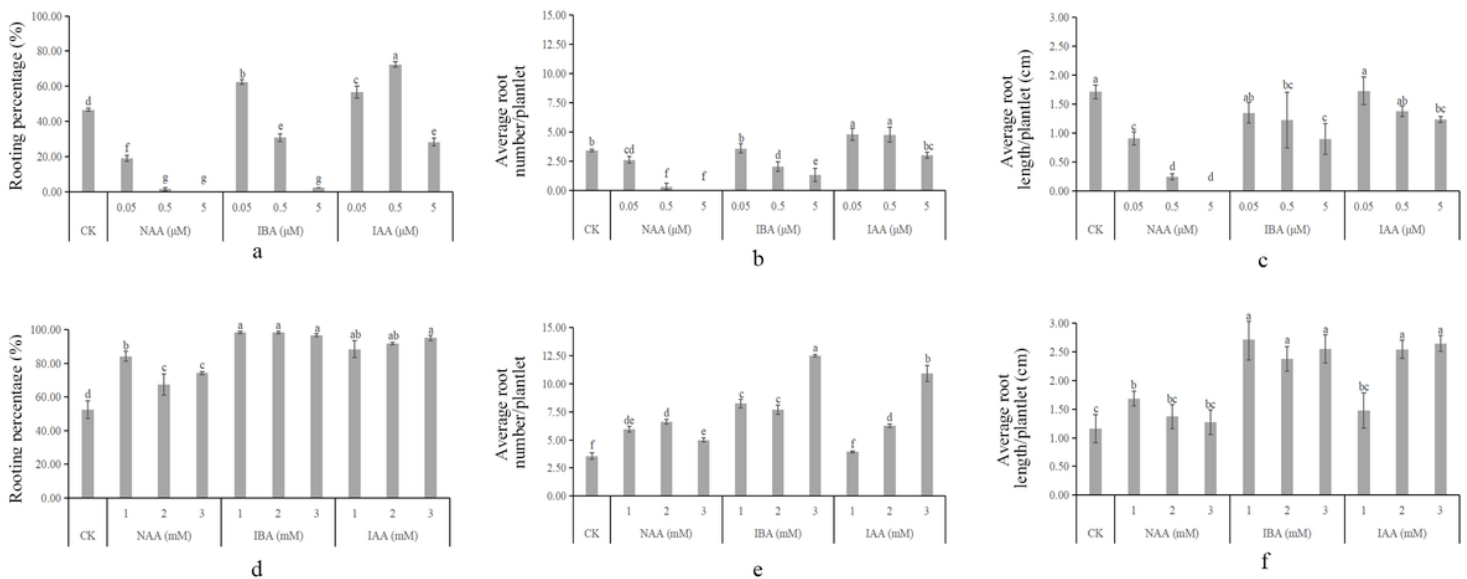


Figure 1

Adventitious root induction of *Euryodendron excelsum* shoots during in vitro rooting at 60 d (a, rooting percentage; b, root number; c, root length) and ex vitro rooting at 25 d (d, rooting percentage; e, root number; f, root length) after treatment. Bars indicate means ± SE. Different letters indicate statistically significant differences compared with the control (CK) based on Duncan's multiple range test (P < 0.05) for the designated treatments. Forty shoots were prepared for each treatment, and three replicates were performed for each treatment.

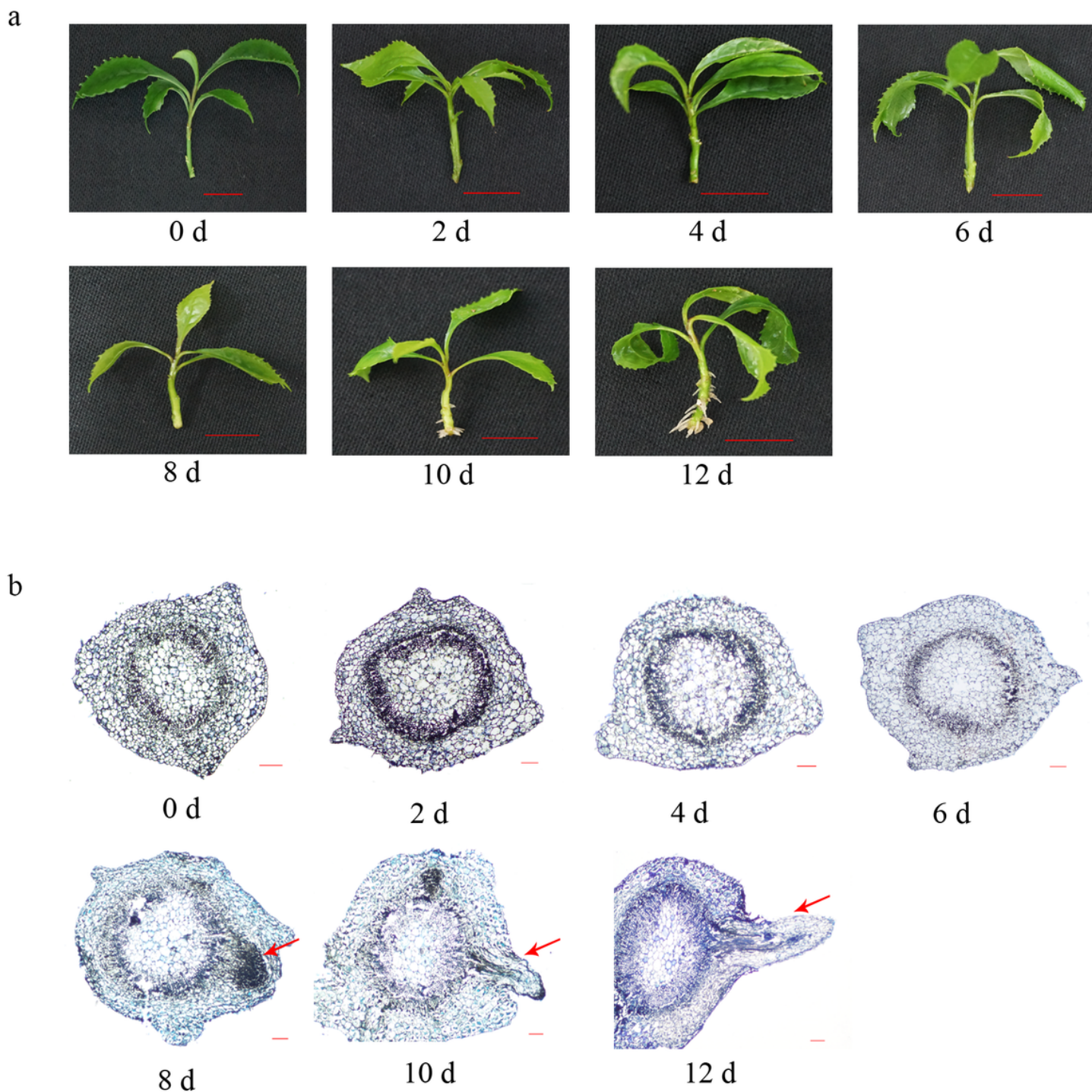


Figure 2

Adventitious root development of *Euryodendron excelsum* shoots from 0 to 12 d after 1 mM IBA treatment during ex vitro rooting. (a) Phenotypic changes between 0 and 12 d after treatment. Red bars = 1 cm. (b) Anatomy of adventitious root development from 0 to 12 d after treatment. Red bars = 0.1 mm. Red arrows indicate the root primordium (8 d) and adventitious roots (10 d and 12 d).

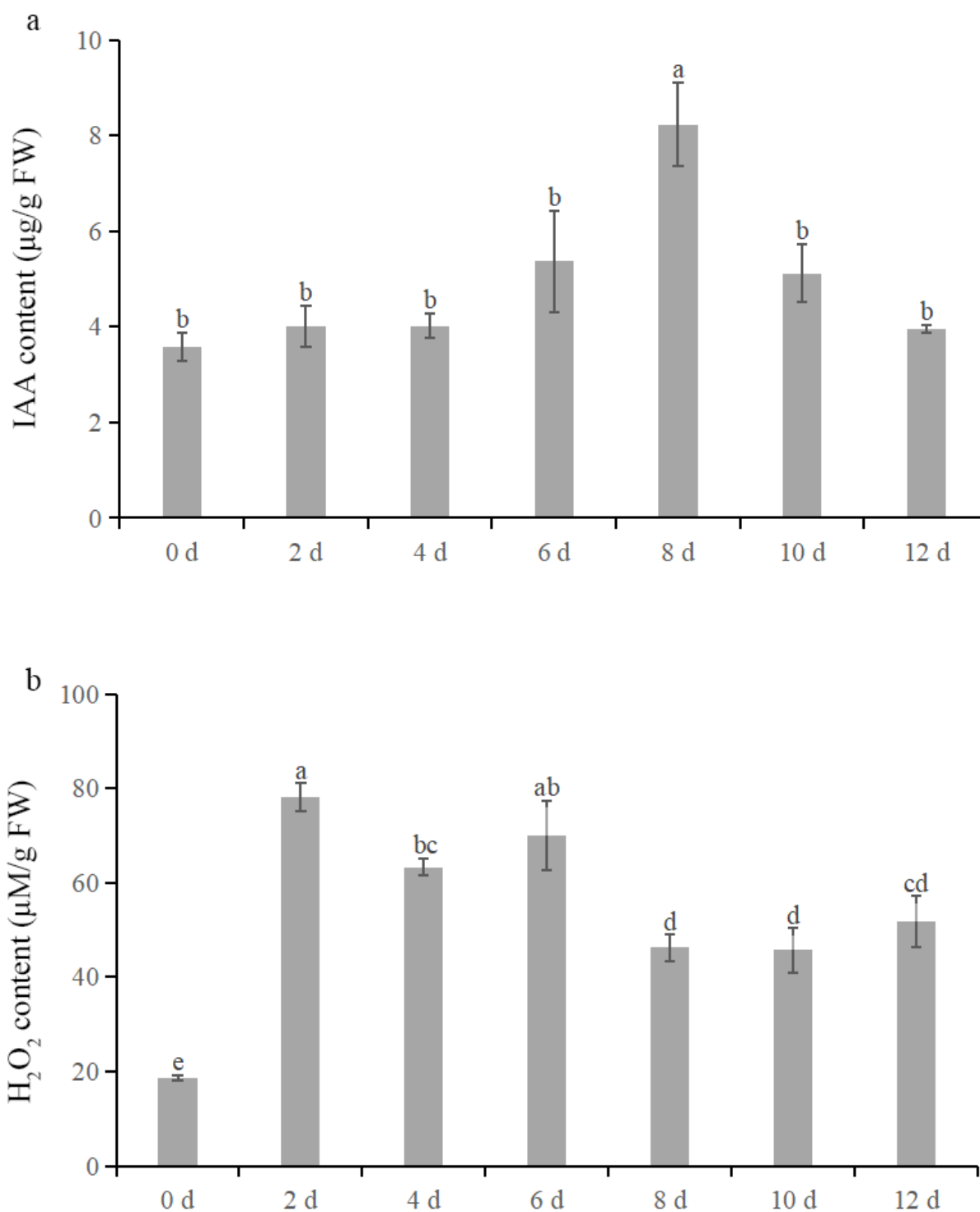


Figure 3

Determination of endogenous IAA (a) and H₂O₂ (b) content in stem bases of *Euryodendron excelsum*. Bars indicate means ± SE. Different letters indicate statistically significant differences compared with the control (0 d) based on Duncan's multiple range test (P < 0.05) for the designated treatments. Three biological replicates of 10 cut stem bases were harvested as 0.1 g fresh weight (FW) to assess endogenous IAA and H₂O₂ content.

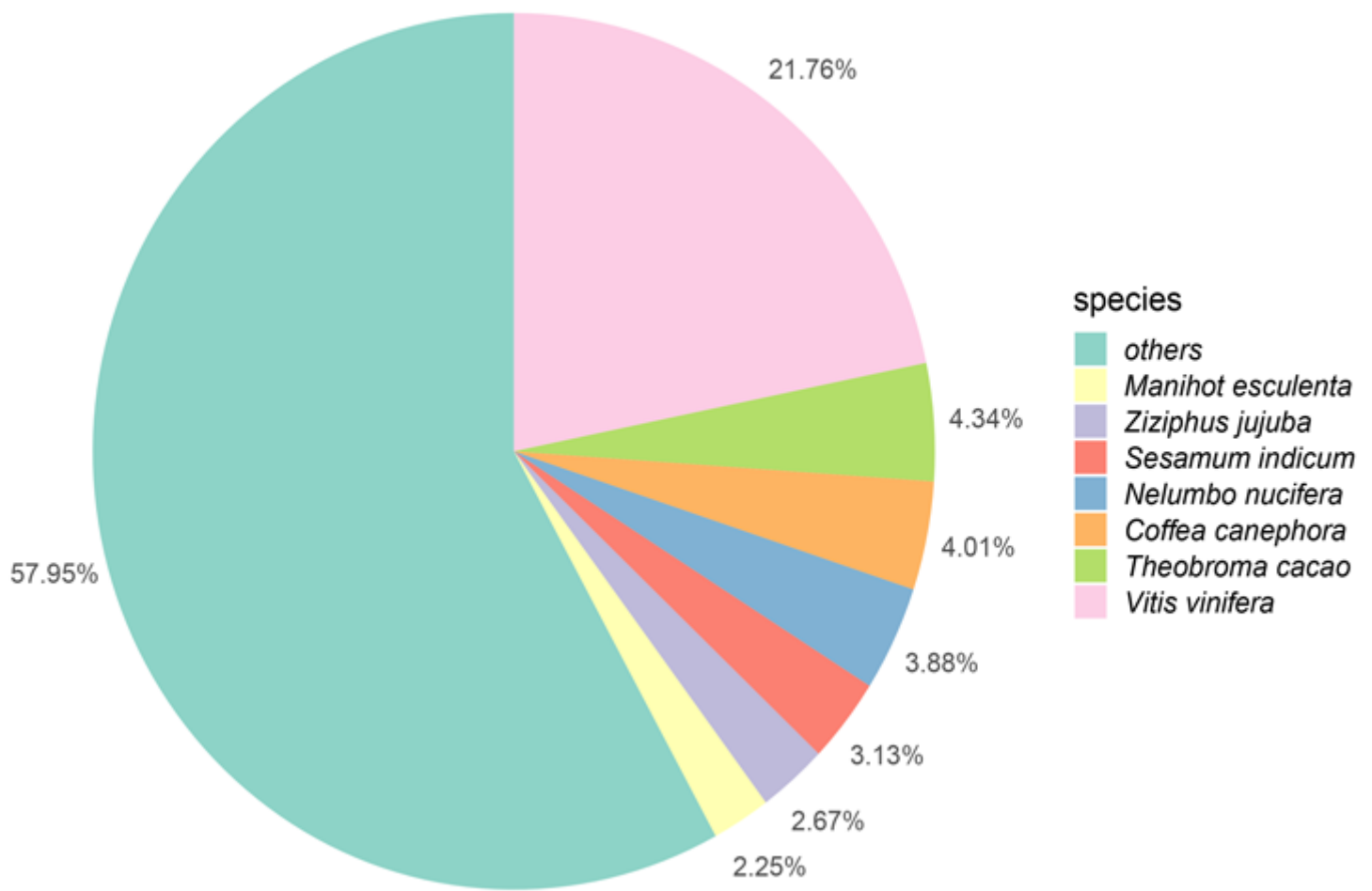


Figure 4

Species distribution of the top BLAST hits against the NR database in *Euryodendron excelsum*. Pie charts were generated by R software.

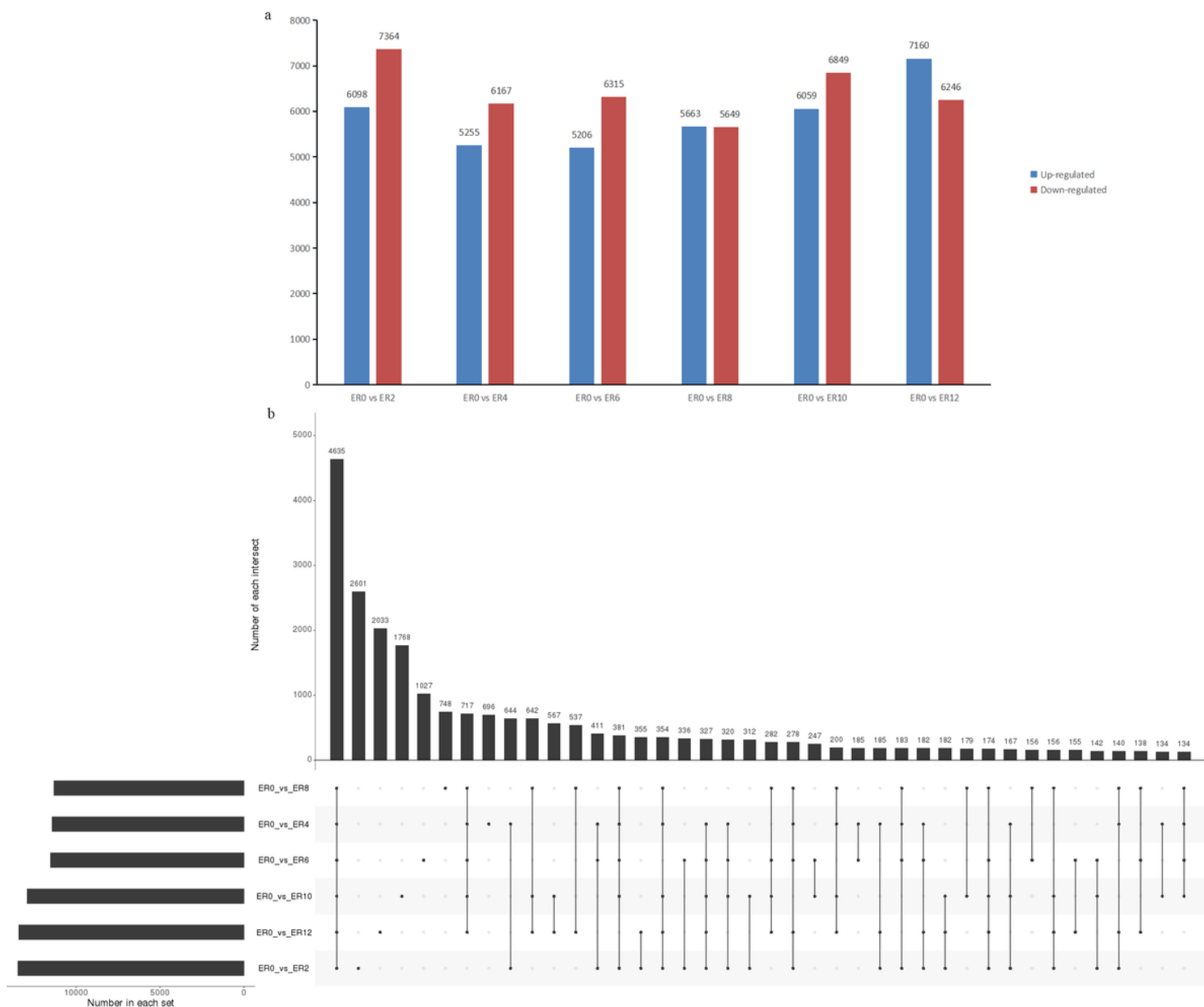


Figure 5

Number of DEGs and Upset plot diagram analysis of DEGs during adventitious root development of *Euryodendron excelsum*. Upset plot diagram was generated by R software. (a) Number of up- and down-regulated DEGs in 2 (ER2), 4 (ER4), 6 (ER6), 8 (ER8), 10 (ER10) and 12 (ER12) d treatments compared with 0 d (ER0). The x-axis represents the time point after IBA treatment during ex vitro rooting, while the y-axis represents the number of DEGs; (b) Upset plot diagram analysis of the DEGs. The connections on the x-axis between points in vertical lines represent the intersection between corresponding data sets, while the y-axis represents the number of DEGs in each intersection.

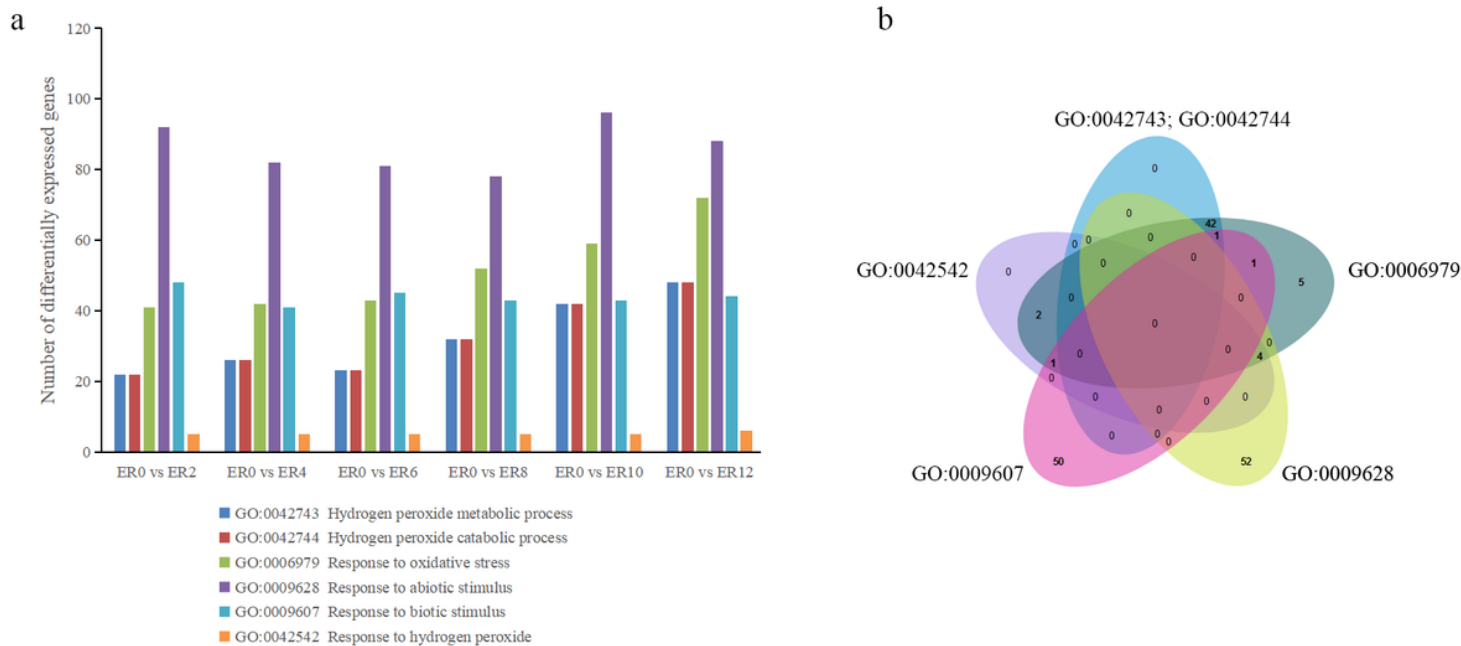


Figure 6

DEGs related to adversity stress in GO enrichment analysis. (a) Number and categories of DEGs. (b) Venn diagram analysis of up-regulated DEGs related to adversity stress.

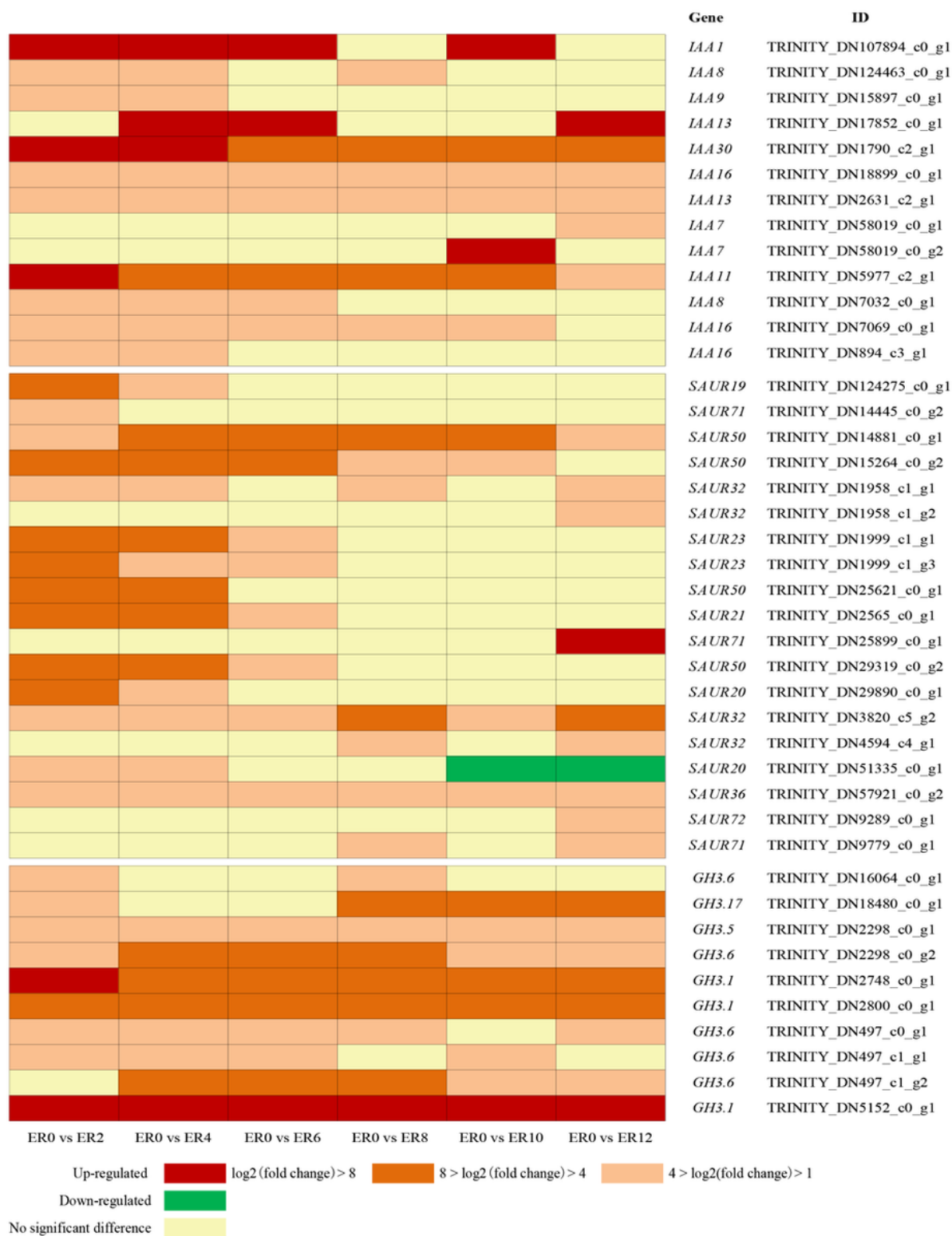


Figure 7

Analysis of the fold changes of up-regulated genes related to AUX/IAA, SAUR and GH3 in *Euryodendron excelsum* determined by RNA-seq. Graphs were generated by Microsoft Excel and Adobe Photoshop CC 2018.

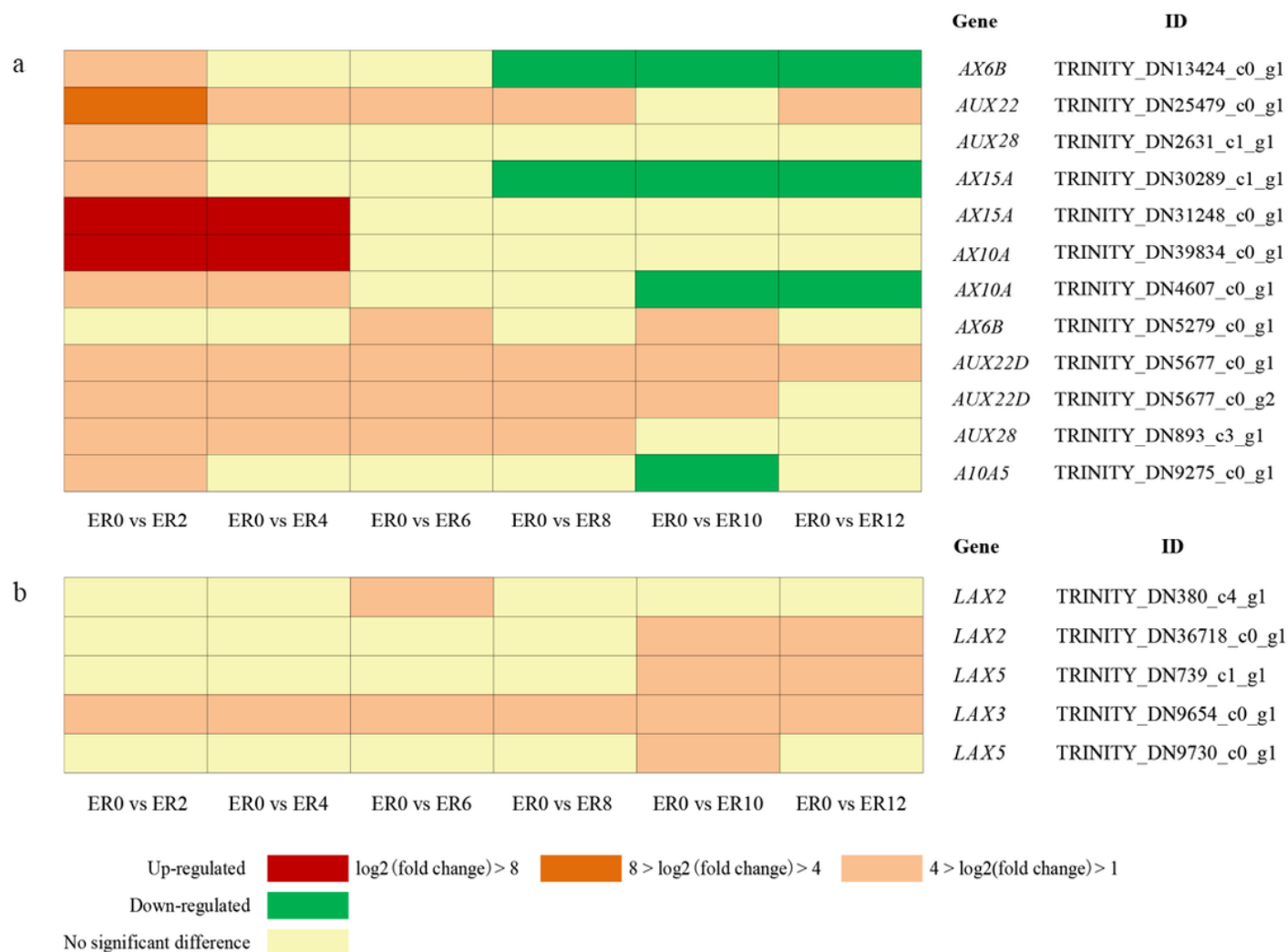


Figure 8

Analysis of the fold changes of up-regulated genes related to AUX (a) and AUX1/LAX (b) during adventitious root development of *Euryodendron excelsum* determined by RNA-seq. Graphs were generated by Microsoft Excel and Adobe Photoshop CC 2018.

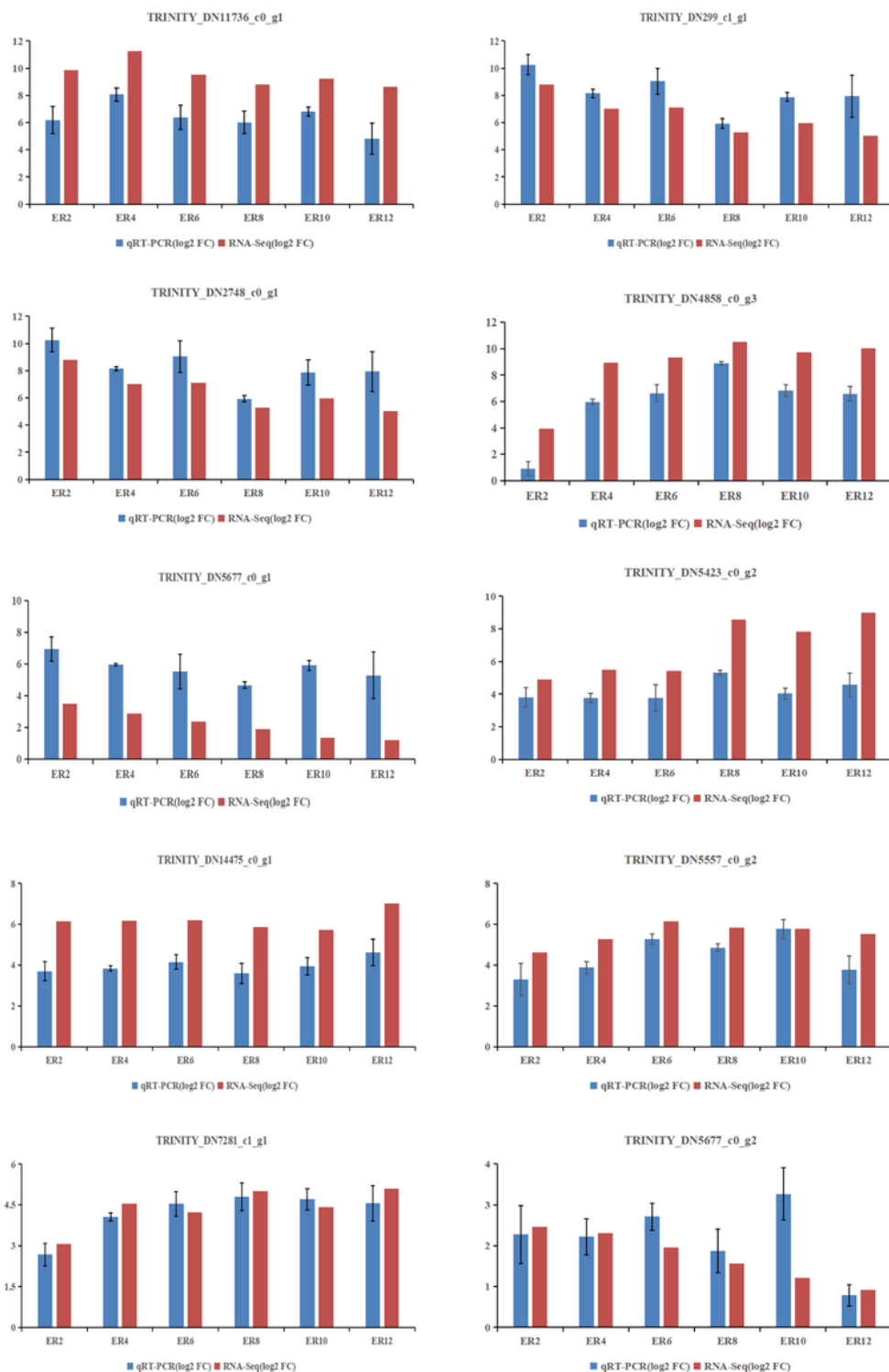


Figure 9

Analysis of the fold changes of 10 candidate genes in *Eurydendron excelsum* determined by RNA-seq and qRT-PCR. Bars indicate means \pm SD. The x-axis represents the time point after each treatment while the y-axis represents the log2(fold change). Graphs were generated by Microsoft Excel and Adobe Photoshop CC 2018.

Supplementary Files

This is a list of supplementary files associated with this preprint. Click to download.

- [FigureS1.tif](#)
- [FigureS2.tif](#)
- [FigureS3.tif](#)
- [FigureS4.tif](#)
- [FigureS5.tif](#)
- [FigureS6.tif](#)
- [FigureS7.tif](#)
- [TableS1.xlsx](#)
- [TableS2.xlsx](#)
- [TableS3.xlsx](#)
- [Table1.pdf](#)
- [Table2.pdf](#)